Published in final edited form as:
Spine (Phila Pa 1976). 2009 February 15; 34(4): 309–315. doi:10.1097/BRS.0b013e318191ea01.

Anatomical and Biomechanical Analyses of the Unique and Consistent Locations of Sacral Insufficiency Fractures

Nathan J. Linstrom, MD[1], **Joseph E. Heiserman, MD, PhD**[1], **Keith E. Kortman, MD**[2], **Neil R. Crawford, PhD**[3,4], **Seungwon Baek, MS**[3], **Russell L. Anderson, MS**[4], **Alan M. Pitt, MD**[1], **John Karis, MD**[1], **Jeff S. Ross, MD**[1], **Gregory P. Lekovic, MD, JD**[5], and **Bruce L. Dean, MD**[1]

[1]Institutions: Barrow Neurological Institute St Joseph Hospital and Medical Center 350 West Thomas Road Phoenix, AZ 85013

[2]Chief of Radiology Sharp Memorial Hospital 7901 Frost Street San Diego, California 92123

[3]Spinal Biomechanics Laboratory Barrow Neurological Institute

[4]Arizona State University Harrington Department of Bioengineering Tempe, Arizona 85287

[5]Department of Neurological Surgery Barrow Neurological Institute

Abstract

Study Design—Correlation of locations of sacral insufficiency fractures are made to regions of stress depicted by finite element analysis derived from biomechanical models of patient activities.

Objective—Sacral insufficiency fractures occur at consistent locations. It was postulated that sacral anatomy and sites of stress within the sacrum with routine activities in the setting of osteoporosis are foundations for determining patterns for the majority of sacral insufficiency fractures.

Summary of Background Data—The predominant vertical components of sacral insufficiency fractures most frequently occur bilaterally through the alar regions of the sacrum which are the thickest and most robust appearing portions of the sacrum instead of subjacent to the central sacrum which bears the downward force of the spine.

Methods—First, the exact locations of 108 cases of sacral insufficiency fractures were catalogued and compared to sacral anatomy. Second, different routine activities were simulated by pelvic models from CT scans of the pelvis and finite element analysis. Analyses were done to correlate sites of stress with activities within the sacrum and pelvis compared to patterns of sacral insufficiency fractures from 108 cases.

Results—The sites of stress depicted by the finite element analysis walking model strongly correlated with identical locations for most sacral and pelvic insufficiency fractures. Consistent patterns of sacral insufficiency fractures emerged from the 108 cases and a biomechanical classification system is introduced. Additionally, alteration of walking mechanics and asymmetric sacral stress may alter the pattern of sacral insufficiency fractures noted with hip pathology (p=.002).

Conclusions—Locations of sacral insufficiency fractures are nearly congruous with stress depicted by walking biomechanical models. Knowledge of stress locations with activities, cortical bone transmission of stress, usual fracture patterns, intensity of sacral stress with different activities, and modifiers of walking mechanics may aid medical management, interventional, or surgical efforts.

Correspondence: Bruce L. Dean, MD Barrow Neurological Institute St. Joseph Hospital and Medical Center 350 West Thomas Rd. Phoenix, AZ 85013 phone - 602 406-3430 fax - 602 957-6142 email - E-mail: bdean@sniweb.net.

Expedited IRB approval for the study was obtained.

Keywords

Sacrum; Insufficiency Fractures; Finite Element Analysis; Classification System; Biomechanics

Key Points

- Identify the exact locations of sacral insufficiency fractures from large a consecutive series of cases by MRI and/or CT anatomical imaging methods.
- Biomechanical model simulations to determine locations of stress within the sacrum with patient activities determined by finite element analysis.
- Match clinical locations of sacral insufficiency fractures and sacral stress with activities as identified by the biomechanical models.
- Sacral insufficiency fracture biomechanical classification system is introduced.
- Knowledge of sacral stress locations with activities, cortical bone transmission of stress, usual sacral insufficiency fracture patterns, intensity of sacral stress with different activities, and modifiers of walking mechanics may aid medical, interventional, or surgical management of patients.

Introduction

Osteoporotic sacral insufficiency fractures may present with characteristic “H” type patterns with both vertical and horizontal components of fractures across the sacrum; bilateral or unilateral vertical fractures through the sacral alar regions medial to the sacroiliac joints and lateral to the neuroforamena; isolated horizontal components; or variations of these patterns.

In contrast, post-traumatic non-osteoporotic sacral fractures occur at many different locations throughout the sacrum including the neuroforamena and central canal and are more commonly unilateral when there is a vertical component(1-6). Insufficiency (7-14) fractures may present with bilateral vertical alar components with the “H” pattern the most common pattern in most published series(12,15,16), but a single unilateral vertical component is common and is the most common pattern in a smaller number of series (17,18). Regardless, the vertical components nearly invariably involve the alar regions of the sacrum medial to the sacroiliac joints.

It is counterintuitive that the vertical components of sacral insufficiency fractures most consistently occur through the thickest and most robust appearing portion of the sacrum adjacent to the sacroiliac joints instead of medially where the sacrum bears the weight of the spine and upper body, and has thinner AP dimensions. We hypothesized that sacral anatomy and the location of stress within the sacrum with routine activities are the foundations for consistent locations for most sacral insufficiency fractures, and are the predominant causes of sacral insufficiency fractures in the setting of osteoporosis.

The first component of this study was to identify and catalogue the exact locations of sacral insufficiency fractures from CT or MRI scans from a group of 108 patients with sacral insufficiency fractures. These fracture locations were then compared to anatomical features of the sacrum that may predispose the sacrum to fracture planes in the setting of osteoporosis.

The second component of the study was composed of biomechanical analyses of the sacrum. Finite element analyses were performed on 3D computer models of the pelvis and sacrum to highlight stress within the sacrum. Different patient activities and their effects on the sacrum were simulated by altering forces and boundary conditions for finite element analysis.

Materials and Methods

Anatomical Analysis

The retrospective format of the clinical portion of the study qualified the study for expedited IRB approval and waiver of consent. Patient identification data were protected by the primary investigators.

One hundred and eight sets of imaging studies from patients with sacral insufficiency fractures were retrospectively reviewed. Sixty six cases from 2001 to 2006 were from institution #1 and 42 cases from 2003 to 2006 were from institution #2. Additional clinical information was obtained from patient charts and imaging reports. Findings or histories that could potentially alter the location of sacral insufficiency fractures by focal sacral structural or non-uniform material properties were noted, and these cases were assigned to the “Modified Biomechanics” group or excluded from the study. This group also included cases with prior pelvic radiation, Tarlov cysts, small sacral masses, and uncommon or unusual fracture patterns.

Our intent was to limit study cases to insufficiency fractures caused by cyclic loading of osteoporotic bone and prevent inclusion of pathologic and post-traumatic fractures masquerading as insufficiency fractures. Exclusionary criteria for the study included large focal masses of the sacrum and resultant pathologic fractures, prior sacral surgery, and Paget's disease. Cases with clear history of trauma or numerous synchronous rib or extremity fractures at other locations of the body were considered post-traumatic fractures and excluded from the study.

The 108 cases were divided into two datasets. Group 1 cases were presumed to be osteoporotic sacral insufficiency fractures and fracture planes were determined by sacral anatomy and sacral stress with activities. Group 2 cases had pre-existing potentially confounding small sacral lesions, altered regional bone material properties, or unusual biomechanics that could alter the common locations of insufficiency fractures. All imaging studies were reviewed by at least two senior Neuroradiologists (BD, AP, JR, and KK) for agreement of fracture locations. Over 1,000 MRIs, CTs, bone scans, or additional imaging studies were reviewed from the 108 patients. Identification of exact locations of insufficiency fractures was limited to CTs and MRIs because of their higher anatomic resolution.

After review of all 108 cases, 85 cases were assigned to Group 1 and were presumed to have osteoporotic insufficiency fractures with at least one adequate CT or MRI of the pelvis or lumbosacral spine which included the sacrum. Osteoporosis was confirmed in Group1 patients by history, imaging, or bone mineral densities. Twenty three cases were assigned to the Group 2, “Modified Biomechanics” category because of confounding factors that could possibly alter the location of the insufficiency fractures or unusual biomechanics.

Also, an association was suspected between unilateral vertical asymmetric sacral insufficiency fractures caused by altered mechanics with activities of Group1 patients and hip pathology. The hip pathology could potentially subject the sacrum to asymmetric stress and could be identified on lumbosacral spine CTs or MRIs. The null hypothesis was the association was random. One-tailed 2×2 Fisher exact test was used to evaluate random association between asymmetric sacral insufficiency fractures and hip pathology.

Biomechanical Analyses

The biomechanical portion of the study used computer 3D models for finite element analysis to identify stress locations by ANSYS (ANSYS, Inc., Canonsburg, PA). The 3D models were prepared and meshed prior to the ANSYS finite element analysis. One model introduced repetitive vertical loading over the central sacrum to simulate bipedal weight bearing and

stationary activities with boundary conditions composed of constraints at both acetabula (Fig. 1). A second clinical model was tested with alternating weight bearing of the two sides of the pelvis to simulate walking, stair-climbing, and jogging (Fig. 2). A third clinical model simulating pre-existing partial vertical sacral alar fractures was tested to evaluate transverse component fracture occurrence (Fig. 3) after vertical component fractures.

The finite element mesh was patterned after the pelvic bone models proposed by Dalstra and Phillips(19). Separate ROIs (regions of interest) were delineated for cortical and cancellous bone regions. Cortical bone was meshed with shell elements and cancellous bone with 10 node tetrahedral elements. Different material properties were assigned to each. Cortical bone elastic modulus was E= 12 GPa (gigapascals, kN/mm^2). Poisson's ratio was $\upsilon = 0.3$. Cancellous bone material properties were set at E = 100 MPa (megapascals) and $\upsilon = 0.2$. Constant cortical thickness (0.45 mm) and nonlinear material properties were assumed. Sacral loads were applied over the S1 body. Physiologic loads of 400, 800, and 1200 Newtons were applied to the sacrum to simulate different levels of activities, although stress patterns should be similar for different loads, but different intensities. Four hundred Newtons is equivalent to approximately 90 pounds weight for the pelvis, abdomen, and upper body. Inter-pubic ligament (10 node tetrahedral mesh) properties were E = 12 MPa and $\upsilon = 0.45$. Pelvic model finite element meshes were composed of 108,339 cortical and 681,505 cancellous elements. The computations were performed on a 4 CPU (Intel) computer with 16 gigabytes of RAM. Solutions of models required approximately 1.5 hours of computational time for each model.

Results

Anatomical Data

There were 85 Group 1 conventional osteoporotic cases and the mean age of Group 1 osteoporotic cohort was 76.8 years. Seventy nine of 85 were females (92.9%) and 6 of 85 were males (7.1%). The range of ages spanned 26 to 95 years. The mean age for the 79 females was 76.9 years and 77.3 years for the 6 males.

Common insufficiency fracture patterns emerged from the series of 108 cases. Group 1 cases had normal underlying sacral anatomy and were presumed to have uniform but osteoporotic bone material properties. Group 1 cases were further divided into two categories composed of symmetric and asymmetric fracture patterns. Group 2 cases had pre-existing focal or non-uniform abnormalities that could distort fracture locations (13 with pelvic radiation, 3 small Tarlov cysts, 4 with uncommon transverse-only fracture patterns, and 3 small sacral masses) and presented with advanced or unusual fracture patterns. Thirteen total cases were excluded from analyses. Causes for exclusion were: 3 cases with history of trauma, 4 cases with large sacral masses, 4 cases with inadequate images, one case with prior sacral surgery, and one case with sacral Paget's disease. Figure 4 introduces a biomechanical classification system that can be used to describe this arrangement of fracture patterns. The “H” pattern was most common (Table 1).

Unilateral hip pathology (Fig 5) was noted in 11 of 23 cases with asymmetric vertical sacral fractures. Only 5 of the remaining 62 Group 1 cases had significant unilateral hip pathology, P=.002 (Table 2).

Biomechanical Data

Finite element analyses depicting stress within the sacrum with different activities are presented in Figures 6 and 7. The values for sacral alar stress from our 1200 Newton models for stationary and walking models were 15 and 30 MPa, respectively. Ambulation (alternating weight-bearing, Figure 7) was the activity that had the distribution of stress within the sacrum that

most closely matched the pattern for sacral and pelvic insufficiency fractures; although, there was some minor overlap for sacral fractures with the stationary model at high loads. Although it was not the focus of the study, the walking model also displayed maximal stress at characteristic locations for pelvic insufficiency fractures. Those regions included the acetabular region, pubic and ischial rami, and inner curve of the iliac wing(20-21).

The walking model did not reveal any significant degree of stress at the S1 or S2 horizontal level where the horizontal components of insufficiency fractures occur. The stationary model displayed low levels of stress at those locations even with high loads. The occurrence of transverse stress within the sacrum after loss of lateral support was validated by the partial bilateral sagittal alar fracture model (Fig. 8).

Discussion

To date, our series of 108 patients with sacral insufficiency fractures is the largest reported in the literature. The most common pattern of sacral insufficiency fracture in our series was bilateral vertical parasagittal plane fractures through the sacral ala medial to the sacroiliac joints, but lateral to the neuroforamena and a horizontal component crossing at the upper S2 or lower S1 levels, forming a characteristic “H” pattern (Figure 4, Table 1).

Sacral insufficiency fractures occur consistently at characteristic locations, and are more commonly bilateral in most large series in contrast to the usual unilateral location of non-osteoporotic post-traumatic fractures(1-6,12,15-18); although, minor acute trauma may mimic any fracture pattern in osteoporotic attenuated bone. Additionally, unilateral vertical insufficiency fractures through the sacral ala are common, and unilateral sacral post-traumatic fractures may present in a similar manner and mimic unilateral sacral insufficiency fractures, similar to sacral insufficiency fractures with asymmetric sacral stress. Sacral stress fractures in healthy athletes (22-25) also occur at similar locations in the sacral ala and are likely mediated by similar biomechanics, but at far higher intensities.

Sacral Osteoporosis

The underlying causes of sacral insufficiency fractures are osteoporosis and greater susceptibility to injury with normal repetitive activities and minor trauma. Trabecular bone is more affected by osteoporosis (19;26) than cortical bone but cortical bone is also significantly attenuated; hence the vertebral bodies, pelvis, and sacrum are particularly susceptible to fractures. Bone quality is a term used to describe the overall integrity of the bone structure. It takes osteoporosis into account and additionally includes structural changes which also contribute to bone integrity and its resistance to failure. Osteoporosis is defined as both low bone mass and micro architectural deterioration of bone tissue, and it lowers bone strength, and lowers the yield or failure threshold.

The ratio of trabecular to cortical bone is highest in the sacral alae and lower in the central portion of the sacrum. The central neural portion of the sacrum which appears resistant to insufficiency fractures (excluding the transverse component) has more cortical layers (4 cortical layers) with the additional posterior neural arch which covers the central sacrum. Additionally there are more cortical layers in the neuroforamenal region of the sacrum. The extreme lateral aspect of the sacrum adjacent to the sacroiliac joint is likely protected from fracture by strong sacroiliac ligaments.

Sacral Insufficiency Fracture Patterns

While “H” pattern fractures were most common in our series, unilateral parasagittal sacral fractures were commonly seen in 27% of patients in Group1 (Figure 4). A horizontal

component of fracture appears to develop at a later stage after there is loss of support for the central sacrum from the laterally positioned sagittal plane vertical fractures which progresses to the typical “H” pattern on imaging studies. This concept was first hypothesized by Cooper (13). The loss of lateral sacral alar support causes the entire weight of the upper body to be longitudinally transferred down the central portion of the sacral bodies. In conjunction with the lumbosacral lordosis this produces an anteroinferior vector of force which causes compression and buckling of the anterior sacral vertebral body and occasionally anterolithesis. The pelvic models for stress (Figures 6 and 7) display little or no stress transversely at the upper S2 or lower S1 levels which supports the concept that the transverse component is a later occurrence and transverse stress becomes a factor only after lateral support is lost (Fig. 8). Also isolated transverse only sacral fractures could potentially occur in patients with extreme amounts of sacral lordosis, unusual stress, or advanced osteoporosis (mean age 88.3 years in our series, Fig. 4 - Group 2).

Unilateral sacral fractures in our series were associated with hip pathology p=.002 that would alter the gait (Table 2) and stress in the sacrum. Additionally, lower extremity abnormalities, scoliosis, modifiers of gait, or sacral loading patterns could also potentially contribute to asymmetric sacral stress. Likely, many unilateral post-traumatic fractures are also included in this category in our series and other series from forgotten trauma or a simple stumble without a fall causing higher levels of unilateral sacral stress.

Sacral Biomechanical Models

The walking model stress pattern (Fig. 7) most closely matched the usual bilateral alar stress fracture locations; although, there may be a component of overlap and some contribution from stationary activities. Walking causes alternate weight bearing by the right and then left lower extremities. The ipsilateral hemipelvis and sacrum is supported by the lower extremity while the ipsilateral sacrum bears the weight of the upper body and the opposite non-weight bearing lower extremity similar to a cantilevered truss subjecting the sacral ala to maximal stress. The distribution of stress within the pelvis and sacrum are modified to a degree by the adjacent musculature and soft tissues.

Walking (27) mechanics in humans are efficient, and the excess energy of planting the foot is stored in the stretch of the muscle-tendon units. The foot is planted and the body is literally pole-vaulted over the foot in an inverted pendulum like motion(28,29). The motion is alternated between right and left feet. The ipsilateral sacrum bears the weight of the upper body and opposite lower extremity with a smaller component of stress borne by the anterior pelvic ring. Additionally, forces transmitted downward from the spine to the sacrum with walking are increased 145-207% (27) compared to bipedal stationary activities. The inferiorly transmitted forces from the spine to the sacrum may be up to 400-500% with stair-climbing or slow jogging compared to bipedal activities (27).

Biomechanical models for the pelvis first proposed by Dalstra (19) indicate that the maximal support and distribution of external forces and stress across the pelvis and sacrum (flat bones) are from cortices of bone that conduct stress from one region of support to another and the central trabeculae serve as spacers for the cortical surfaces. This concept has been supported by subsequent investigators(30). This validated biomechanical model has important therapeutic implications. Therapies should allow healing of the cortical surfaces, since weight-bearing forces are predominantly transmitted as stress across the sacrum via the cortices to the SI joints and iliac bone. Also, the healing sacrum and pelvis should have protected weight-bearing and avoidance of higher stress activities for the pelvis and sacrum. Patients with asymmetric sacral stress fractures should be evaluated for gait abnormalities, altered walking mechanics, or history of prior trauma that may cause unilateral sacral alar fractures.

Our chosen parameters for the study and subsequent results parallel most prior biomechanical studies. Myers and Wilson (31) observed that acute osteoporotic vertebral body fractures occur within a 400-2100 Newton range and osteoporotic sacral insufficiency fractures occur at significantly lower levels than acute traumatic fractures. Waite and Mears (32) tested cadaver osteoporotic specimens and discovered acute traumatic sacral fractures occur at 4-5 times body weight. Bozkus and Hanci (33) also utilized finite element analysis to model non-osteoporotic acute sacral fractures caused by a fall from a height with very high impact loads of 10,000 Newtons. The sacral stress was 430 MPa. Both the loads and sacral stress were much higher than in our study.

Limitations

We chose shell and 10-point tetrahedral mesh finite element models which differ from Dalstra's (19) original model. A more accurate mesh was obtained by this method; however, this method has not been verified by strain gauges similar to the original model. Dalstra indicated that the cortical surface of flat bones transfer 50 times as much stress across flat bones compared to trabecular bone. This may overstate stress conveyance in the cortex within the sacral alae, since sacral alae are thicker than the central sacrum and most flat bones, and trabecular bone likely plays a greater supporting role in the sacral ala.

Our models had an incomplete mesh along the inferior surface of the ischial rami which slightly emphasizes the stress near those locations. No accommodation in the models was made for the sacroiliac joints which may allow movement with activities or supporting sacral soft tissues that may alter stress.

Our study limited the cause of asymmetric sacral stress to hip pathology, since this information was available on pelvic and lumbosacral spine CTs and MRIs. Additional unrecognized musculoskeletal abnormalities likely contribute to asymmetric sacral stress and asymmetric fractures.

Differences in the most common patterns of sacral insufficiency fractures noted in different series may be attributed to different referral patterns of patients; different rates of prior hip and lower extremity surgeries or prostheses in different regions of the US and outside the US; unintentional but biased selection of patients; and inclusion of post-traumatic unilateral sacral fractures likely account for differences in percentiles of the most common patterns of sacral fractures noted in different series.

Conclusions

1. The exact locations of osteoporotic sacral insufficiency fractures from our series of 108 cases most precisely matched the maximal sacral stress displayed by the biomechanical model for walking, excluding the transverse component. The sacrum is also subjected to higher stress with walking compared to stationary activities. Although not the focus of the study, the walking model also depicted stress throughout the pelvis at sites characteristic for pelvic insufficiency fractures. These findings support ambulation as the predominant primary activity causing sacral insufficiency fractures in most patients with osteoporosis without a history of trauma.
2. Review of sacral insufficiency fractures from the series of 108 cases displayed consistent fracture patterns and a biomechanical classification system is introduced in Figure 4 with the more common patterns. Biomechanics support the concept that vertical components of “H” type insufficiency fractures initially occur, and the horizontal component forms after lateral support is lost.

3. Knowledge of stress locations, cortical bone transmission of stress, usual fracture patterns, intensity of sacral stress with different activities, and modifiers of walking mechanics may aid medical, interventional, or surgical management.

Acknowledgements

The authors would like to thank J D Bird for sacral 3D models and Deborah Ravin for sacral classification art work.

The submitted manuscript does not contain information about medical devices or drugs. Federal funding was used for the study. This work was partially supported by National Institute of Health, Grant 1R01EB006135-01.

References

1. Mehta S, Auerbach JD, Born CT, et al. Sacral fractures. J Am Acad Orthop Surg 2006;14:656–65. [PubMed: 17077338]
2. Tile M. Acute pelvic fractures: I. Causation and classification. J Am Acad Orthop Surg 1996;4:143–51. [PubMed: 10795049]
3. Isler B, Ganz R. Classification of pelvic ring injuries. Injury 1996;27(suppl 1):S-A3–12.
4. Young JW, Resnik CS. Fracture of the pelvis: current concepts of classification. AJR Am J Roentgenol 1990;155:1169–75. [PubMed: 2122661]
5. Denis F, Davis S, Comfort T. Sacral fractures: an important problem. Retrospective analysis of 236 cases. Clin Orthop Relat Res 1988;227:67–81. [PubMed: 3338224]
6. Letournel E. Pelvic fractures. Injury 1978;10:145–8. [PubMed: 730336]
7. Blake SP, Connors AM. Sacral insufficiency fracture. Br J Radiol 2004;77:891–6. [PubMed: 15483007]
8. Wild A, Jaeger M, Haak H, et al. Sacral insufficiency fracture, an unsuspected cause of low-back pain in elderly women. Arch Orthop Trauma Surg 2002;122:58–60. [PubMed: 11995886]
9. Weber M, Hasler P, Gerber H. Sacral insufficiency fractures as an unsuspected cause of low back pain. Rheumatology (Oxford) 1999;38:90–1. [PubMed: 10334692]
10. Peh WC, Khong PL, Ho WY, et al. Sacral insufficiency fractures. Spectrum of radiological features. Clin Imaging 1995;19:92–101. [PubMed: 7773883]
11. Cotty P, Fouquet B, Mezenge C, et al. Insufficiency fractures of the sacrum. Ten cases and a review of the literature. J Neuroradiol 1989;16:160–71. [PubMed: 2693625]
12. Weber M, Hasler P, Gerber H. Insufficiency fractures of the sacrum. Twenty cases and review of the literature. Spine 1993;18:2507–12. [PubMed: 8303455]
13. Cooper KL, Beabout JW, Swee RG. Insufficiency fractures of the sacrum. Radiology 1985;156:15–20. [PubMed: 4001403]
14. Chen CK, Liang HL, Lai PH, et al. Imaging diagnosis of insufficiency fracture of the sacrum. Zhonghua Yi Xue Za Zhi (Taipei) 1999;62:591–7. [PubMed: 10502849]
15. Finiels H, Finiels PJ, Jacquot JM, et al. Fractures of the sacrum caused by bone insufficiency. Meta-analysis of 508 cases [in French]. Presse Med 1997;26:1568–73. [PubMed: 9452753]
16. Fujii M, Abe K, Hayashi K, et al. Honda sign and variants in patients suspected of having a sacral insufficiency fracture. Clin Nucl Med 2005;30:165–9. [PubMed: 15722819]
17. Hatzl-Griesenhofer M, Pichler R, Huber H, et al. The insufficiency fracture of the sacrum. An often unrecognized cause of low back pain: results of bone scanning in a major hospital [in German]. Nuklearmedizin 2001;40:221–7. [PubMed: 11797511]
18. Schindler OS, Watura R, Cobby M. Sacral insufficiency fractures. J Orthop Surg (Hong Kong) 2007;15:339–46. [PubMed: 18162683]
19. Dalstra M, Huiskes R. Load transfer across the pelvic bone. J Biomech 1995;28:715–24. [PubMed: 7601870]
20. Chary-Valckenaere I, Blum A, Pere P, et al. Insufficiency fractures of the ilium. Rev Rhum Engl Ed 1997;64:542–8. [PubMed: 9385691]
21. Peh WC, Khong PL, Yin Y, et al. Imaging of pelvic insufficiency fractures. Radiographics 1996;16:335–48. [PubMed: 8966291]

22. Major NM, Helms CA. Sacral stress fractures in long-distance runners. AJR Am J Roentgenol 2000;174:727–9. [PubMed: 10701616]

23. Connolly LP, Drubach LA, Connolly SA, et al. Young athletes with low back pain: skeletal scintigraphy of conditions other than pars interarticularis stress. Clin Nucl Med 2004;29:689–93. [PubMed: 15483479]

24. Johnson AW, Weiss CB Jr, Stento K, et al. Stress fractures of the sacrum. An atypical cause of low back pain in the female athlete. Am J Sports Med 2001;29:498–508. [PubMed: 11476393]

25. Shah MK, Stewart GW. Sacral stress fractures: an unusual cause of low back pain in an athlete. Spine 2002;27:E104–8. [PubMed: 11840118]

26. Burge R, Dawson-Hughes B, Solomon DH, et al. Incidence and economic burden of osteoporosis-related fractures in the United States, 2005-2025. J Bone Miner Res 2007;22:465–75. [PubMed: 17144789]

27. Khoo BC, Goh JC, Bose K. A biomechanical model to determine lumbosacral loads during single stance phase in normal gait. Med Eng Phys 1995;17:27–35. [PubMed: 7704340]

28. Massaad F, Lejeune TM, Detrembleur C. The up and down bobbing of human walking: a compromise between muscle work and efficiency. J Physiol 2007;582:789–99. [PubMed: 17463048]

29. Ezquerro F, Simon A, Prado M, et al. Combination of finite element modeling and optimization for the study of lumbar spine biomechanics considering the 3D thorax-pelvis orientation. Med Eng Phys 2004;26:11–22. [PubMed: 14644594]

30. Ulrich D, van Reitbergen B, Weinans H, et al. Finite element analysis of trabecular bone structure: a comparison of image-based meshing techniques. J Biomech 1998;31:1187–92. [PubMed: 9882053]

31. Myers E, Wilson S. Biomechanics of osteoporosis and vertebral fracture. Spine 1997;22(suppl 24): 25S–31S. [PubMed: 9431641]

32. Waites M, Mears S, Mathis J, et al. The strength of the osteoporotic sacrum. Spine 2007;32:E652–5. [PubMed: 17978639]

33. Bozkus H, Hanci M, Sunbuloglu, et al. Finite element method based stress analysis of zone I and II sacral fractures. Ulus Travma Acil Cerrahi Derg 2005;11:189–94. [PubMed: 16100662]

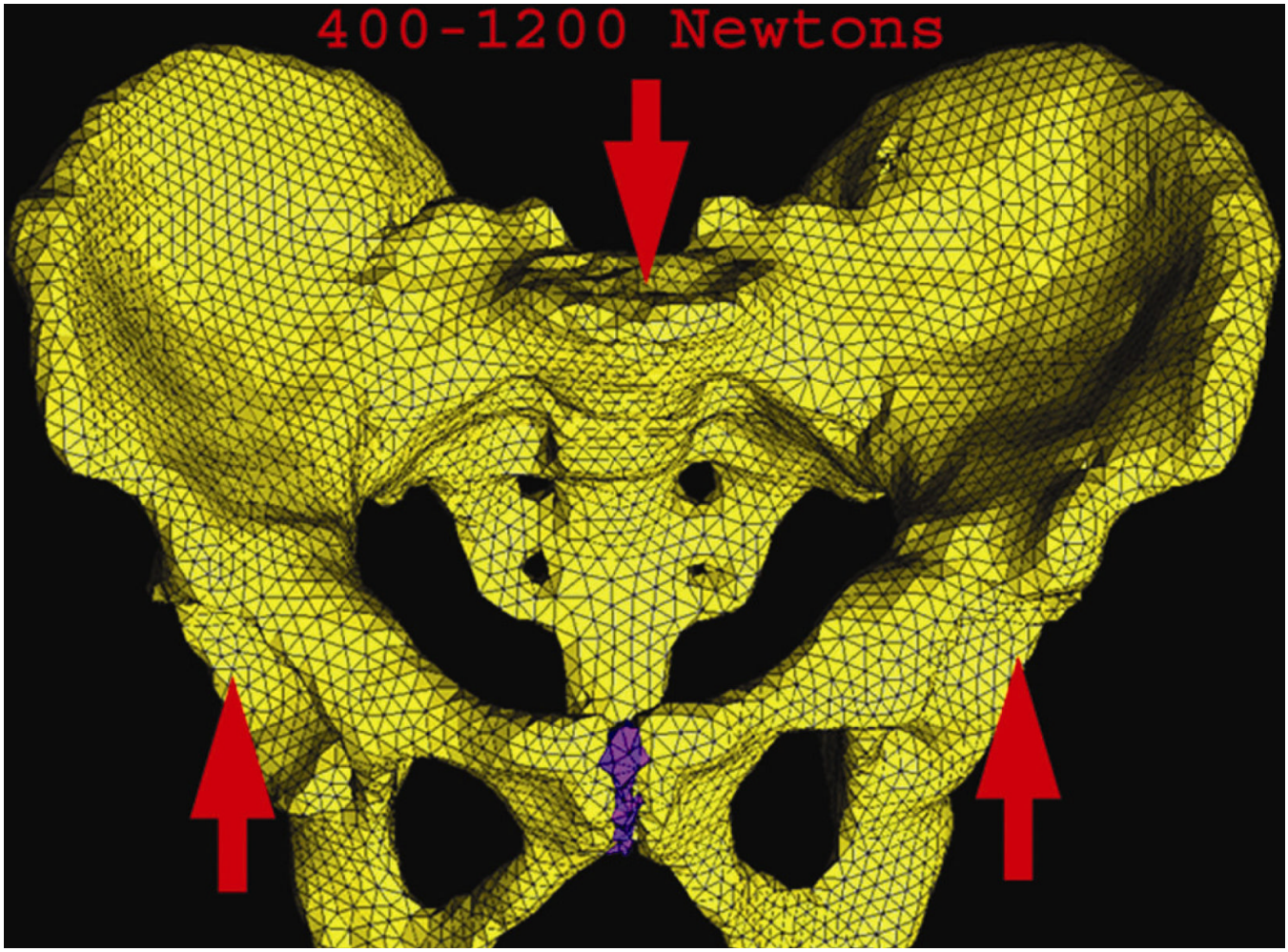

Figure 1.
The biomechanical model was prepared to simulate stationary activities. Finite element meshed model for stationary activities is depicted with 400-1200 Newton loads on the sacrum and bilaterally constrained acetabula.

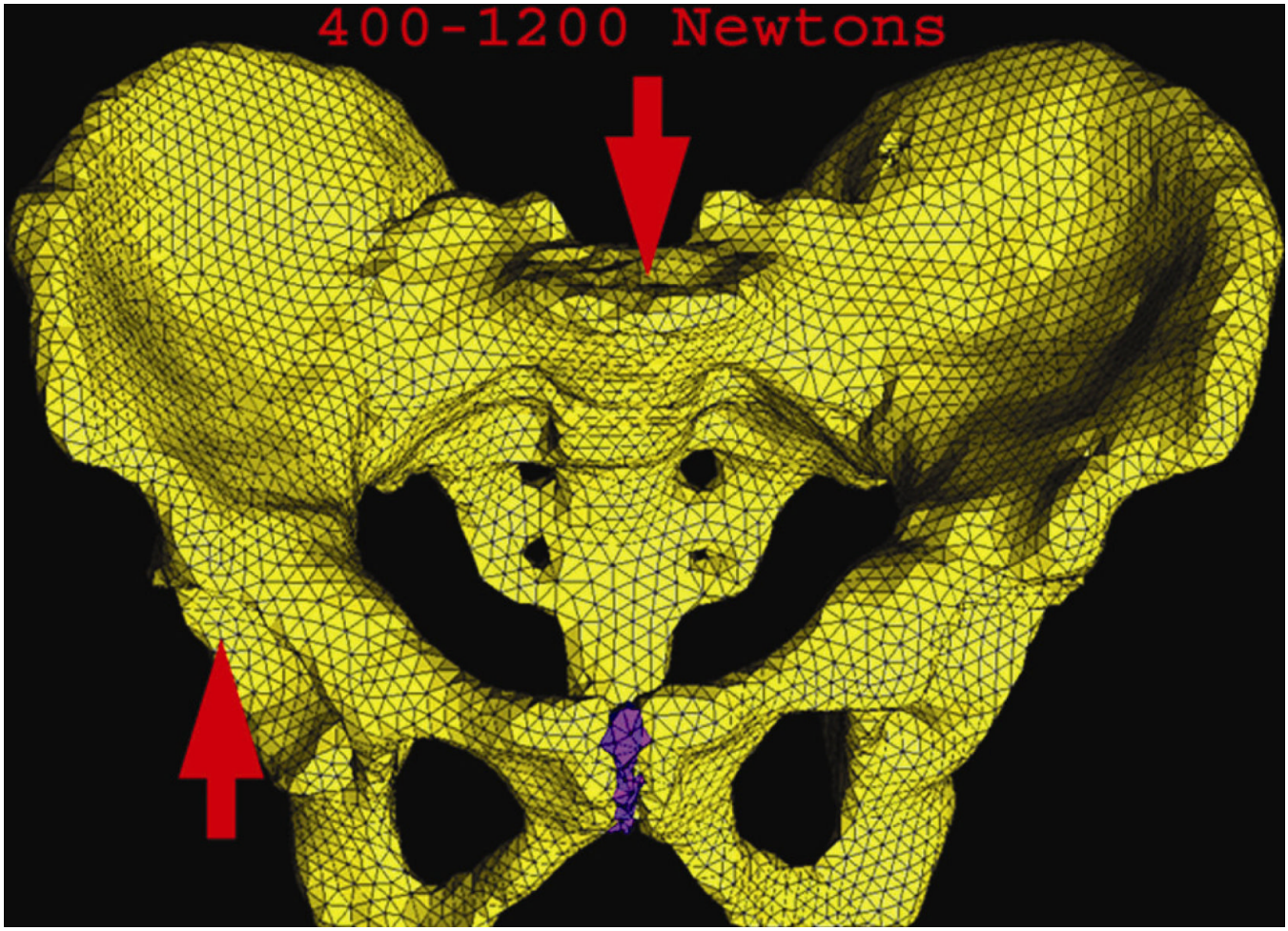

Figure 2.
Meshed model for walking (alternating weight-bearing) is reproduced by applying 400-1200 Newton loads to the sacrum with alternating acetabular constraints.

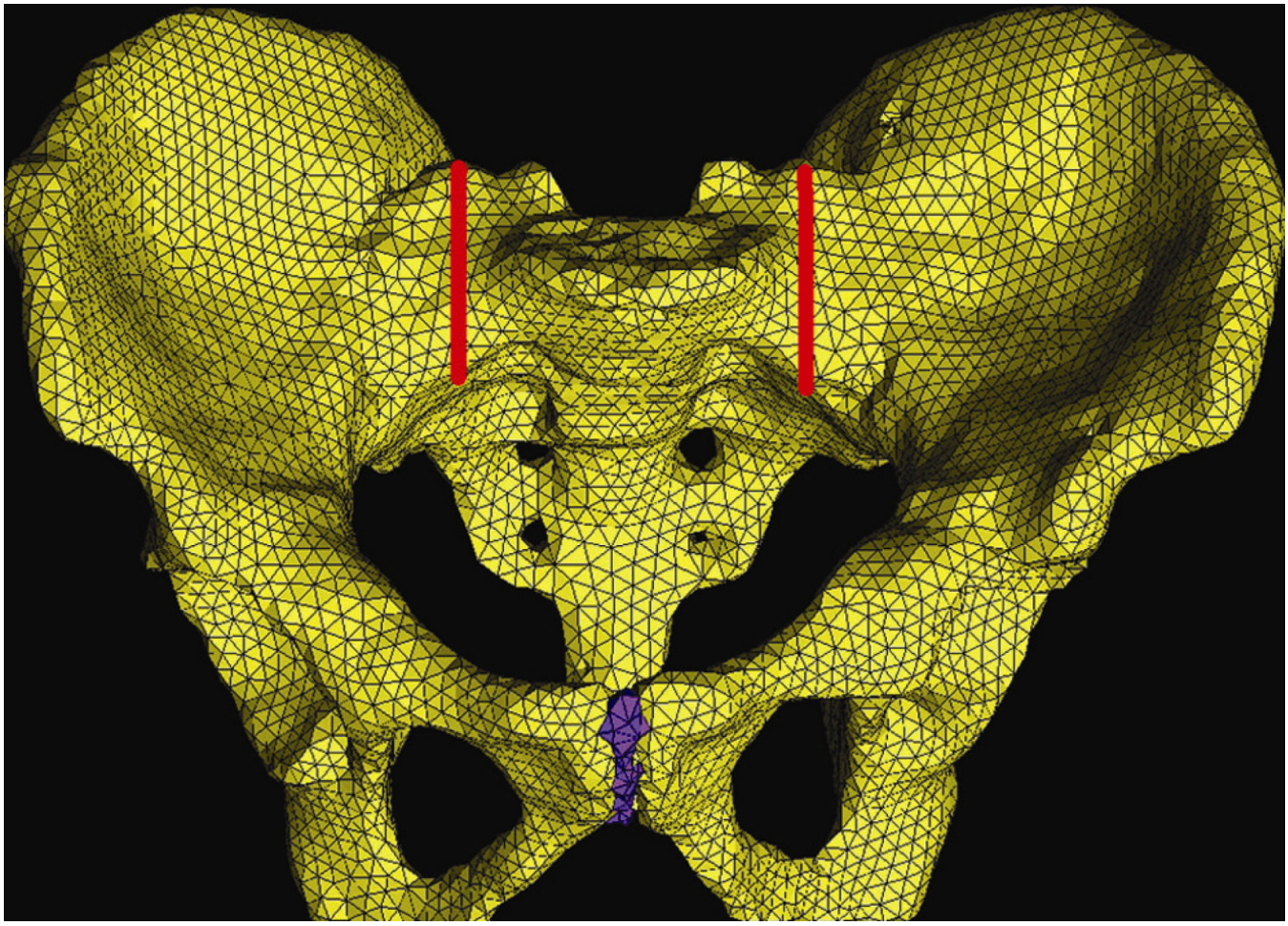

Figure 3.
Vertical red lines simulate partial bilateral vertical fractures of the sacral ala prior to sacral loading.

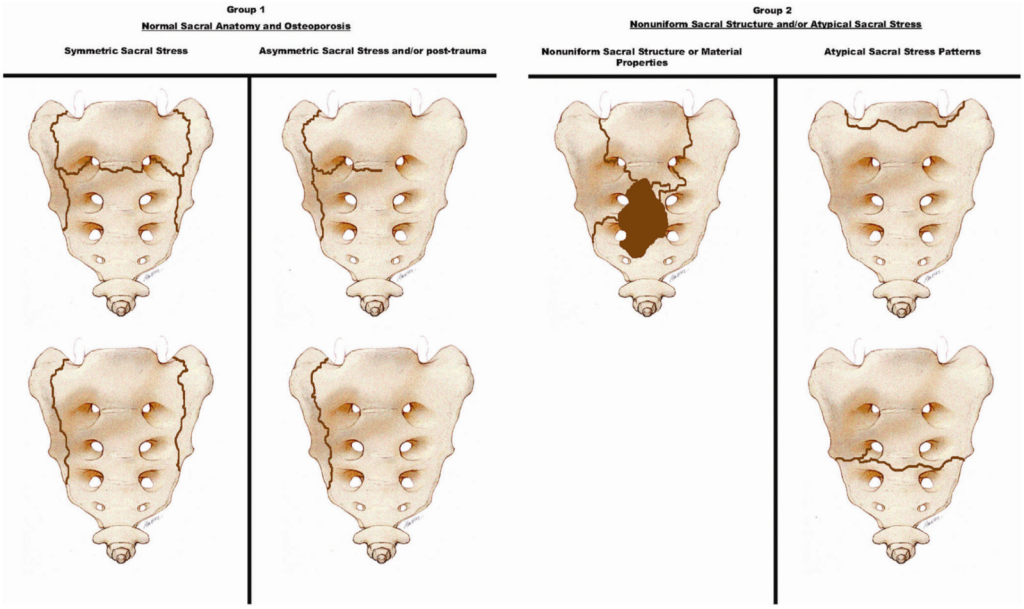

Figure 4.

Common patterns emerged for sacral insufficiency fractures and a biomechanical classification system is introduced. There are two groups. Group 1 cases have normal sacral anatomy and osteoporosis. Group 2 cases have nonuniform material properties, small lesions, or unusual sacral stress patterns.

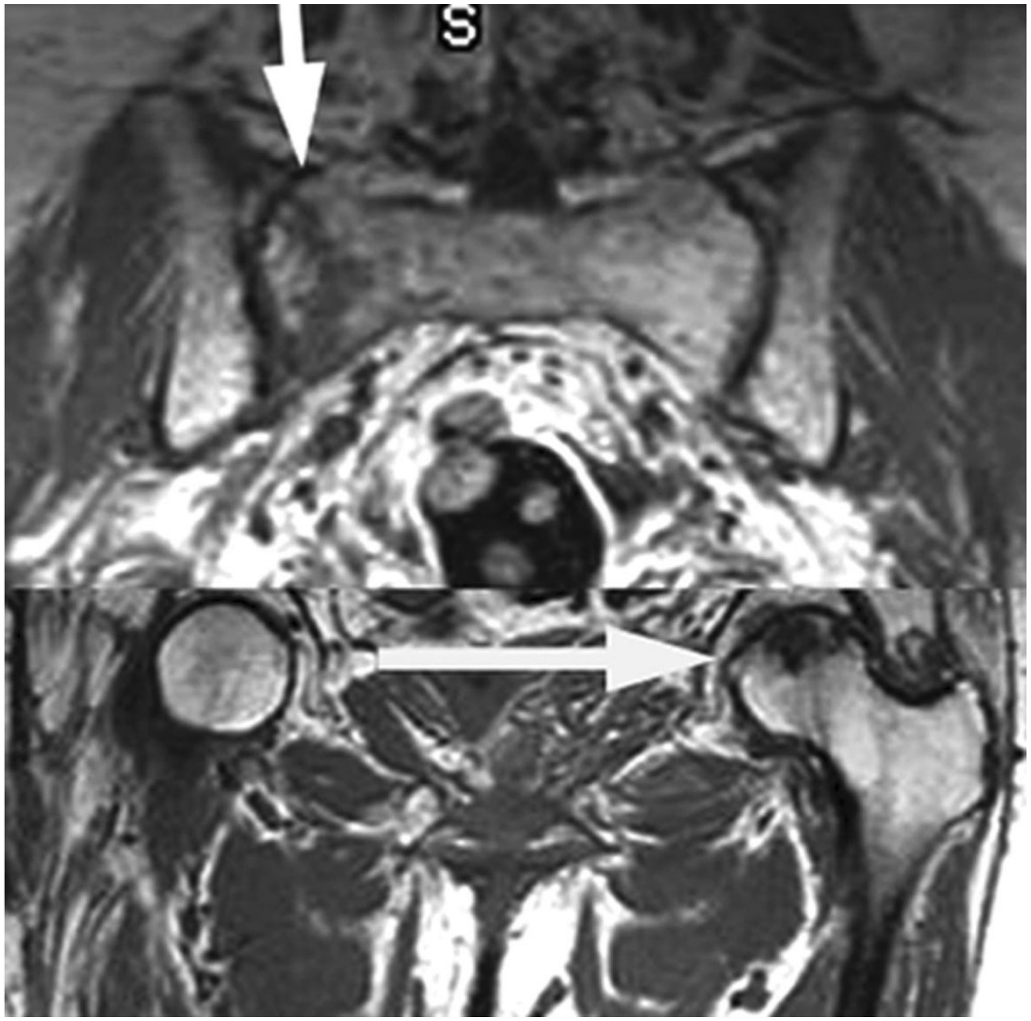

Figure 5.
A merged image from two images from the same MRI sequence in a 68-year-old female displays left hip AVN (long arrow) and a contralateral right vertical sacral insufficiency fracture (short arrow).

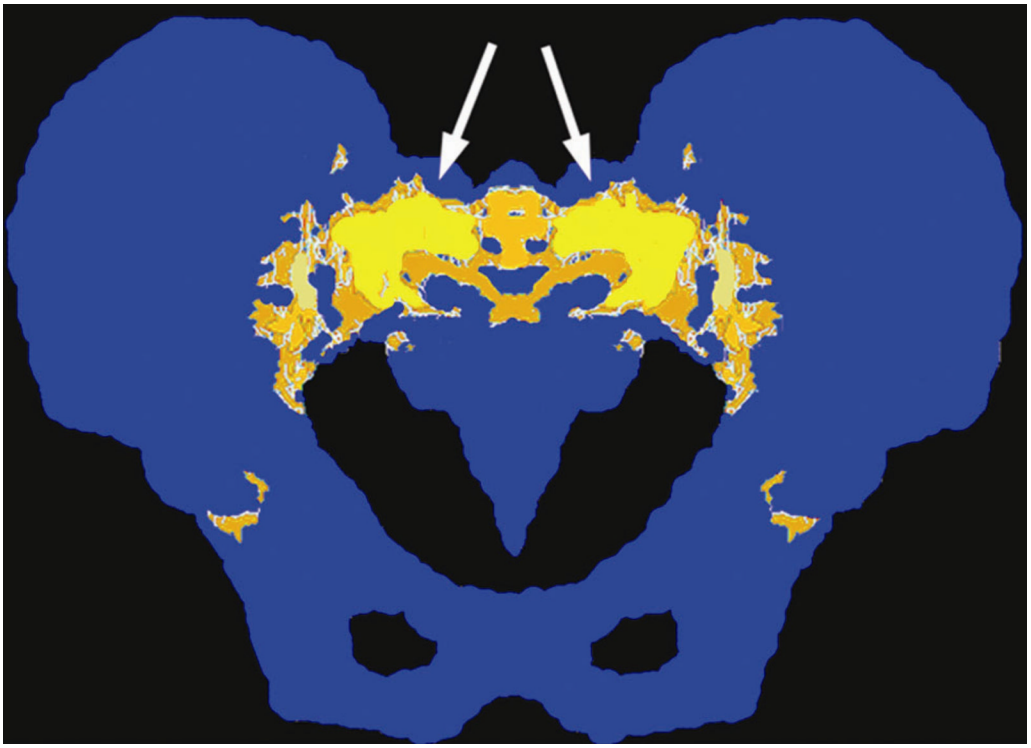

Figure 6.
Solved finite element model with stress indicated by yellow in the sacrum and pelvis. The stationary activity model indicates that stress is maximal (arrows) at the edge of the S1 vertebral body and declines laterally. Brighter shades of yellow indicate higher intensity stress.

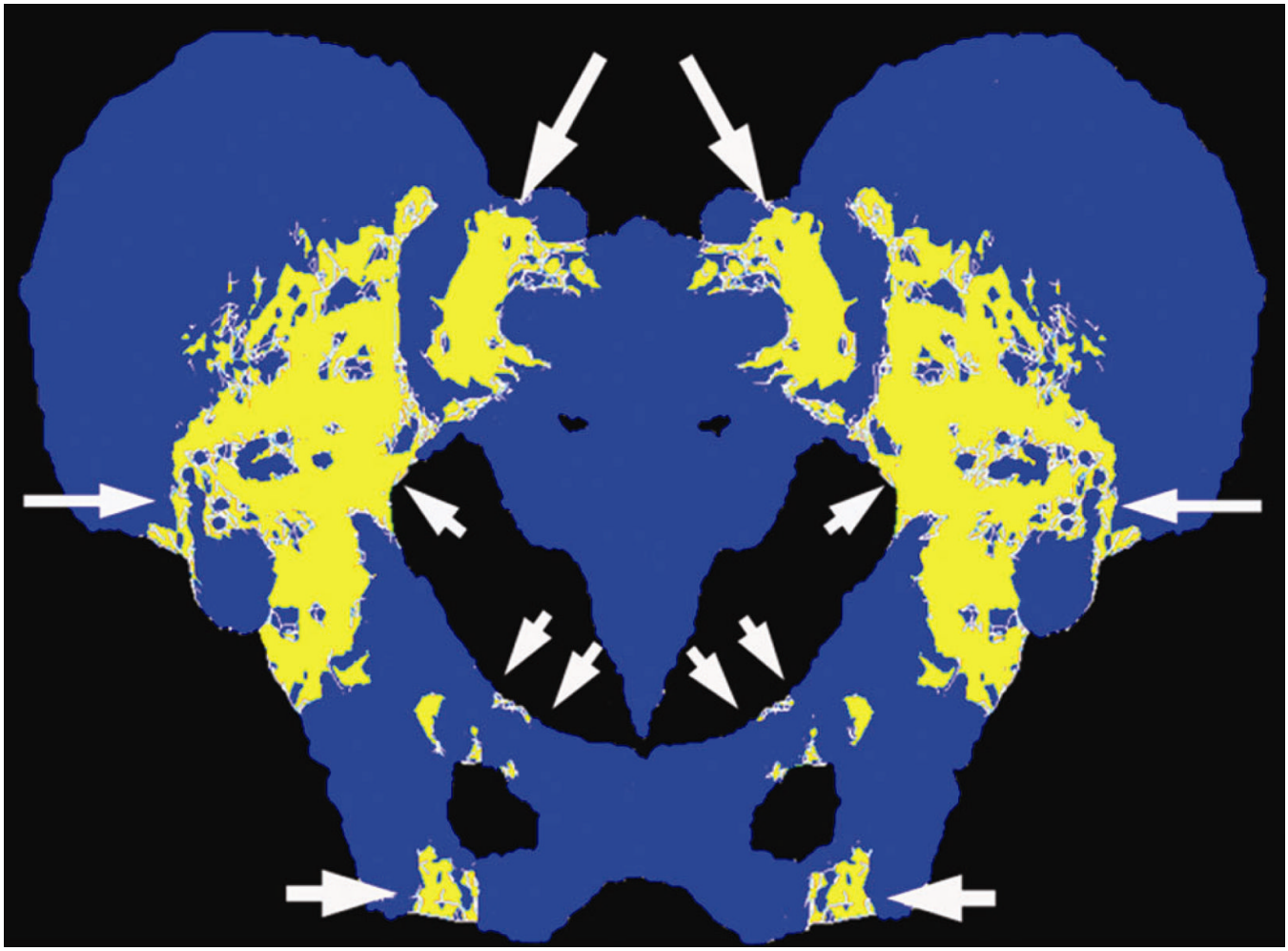

Figure 7.
The walking sacral model displays identical locations for stress compared to vertical sacral insufficiency fracture locations. It also depicts areas of maximal stress throughout the pelvis that also commonly develop insufficiency fractures (arrows).

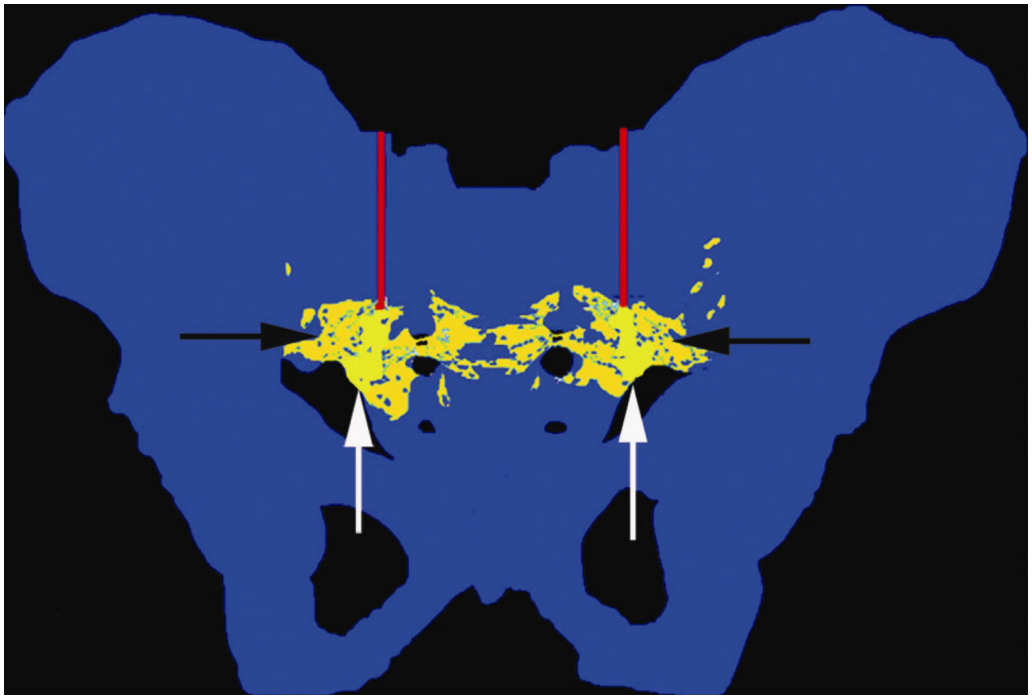

Figure 8.
Vertical alar fractures are simulated by red vertical “cracks” in the model. After loading and loss of lateral support, maximal stress intensities were noted to extend inferiorly (white arrows) to complete the vertical fractures and horizontally (black arrows) to form the transverse component and complete the “H” pattern.

Table 1

Group 1 Osteoporotic Sacrum Most Common Patterns

Most common sacral insufficiency patterns	Percentage of Group 1 cases N = 85
"H" pattern - bilateral vertical plus horizontal components	N = 52 61.2% of total
Unilateral vertical only	N = 16 18.8% of total
Bilateral vertical only	N = 10 11.8% of total
Unilateral vertical plus horizontal component	N = 7 8.2% of total

Table 2

Hip Pathology and Asymmetric Vertical Sacral Fractures

Cases	n = 23 Asymmetric Unilateral Vertical Sacral Fractures	n = 62 Symmetric Bilateral Vertical Sacral Fractures
1	Right hip prosthesis	Right hip prosthesis
2	Right hip prosthesis	Right hip prosthesis
3	Right hip prosthesis	Left hip prosthesis
4	Left hip avascular necrosis	Right hip prosthesis
5	Left hip prosthesis	Right hip prosthesis
6	Right hip prosthesis	N/A
7	Large left hip effusion and severe degenerative joint disease	N/A
8	Left hip avascular necrosis	N/A
9	Left hip prosthesis	N/A
10	Left hip prosthesis	N/A
11	Left hip prosthesis	N/A